

Self-Supervised Object-Level Deep Reinforcement Learning

William Agnew¹ Pedro Domingos¹

Abstract

Current deep reinforcement learning approaches incorporate minimal prior knowledge about the environment, limiting computational and sample efficiency. We incorporate a few object-based priors that humans are known to use: "Infants divide perceptual arrays into units that move as connected wholes, that move separately from one another, that tend to maintain their size and shape over motion, and that tend to act upon each other only on contact" Spelke [1990]. We propose a probabilistic object-based model of environments and use human object priors to develop an efficient self-supervised algorithm for maximum likelihood estimation of the model parameters from observations and for inferring objects directly from the perceptual stream. We then use object features and incorporate object-contact priors to improve the sample efficiency of our object-based RL agent. We evaluate our approach on a subset of the Atari benchmarks, and learn up to four orders of magnitude faster than the standard deep Q-learning network, rendering rapid desktop experiments in this domain feasible. To our knowledge, our system is the first to learn any Atari task in fewer environment interactions than humans.

1. Introduction

Deep reinforcement learning has achieved impressive performance in many environments Mnih et al. [2015, 2016], Silver et al. [2017]. However, the sample inefficiency of deep reinforcement learning algorithms limits applicability to real-world domains. These algorithms are very general, in theory capable of learning in all environments. We are only interested in real-world environments though, suggesting that current deep reinforcement learning algorithms could

be improved by incorporating additional priors or heuristics.

In most real-world environments, humans are able to achieve good performance after far less experience than machines, pointing to human-inspired priors as a means of improving sample efficiency. Past work has considered perceiving the world in terms of objects as humans do (Diuk et al. [2008], Scholz et al. [2014]), and recent work has focused on creating object state representations without supervision (Goel et al. [2018], Zhu et al. [2018], Greff et al. [2019], Lin et al. [2020]). In this work, we use human object priors to develop a probabilistic object model of environments and a tractable algorithm for inferring an explicit object state representation that jointly maximizes the likelihood of a dynamics model and a reward model.

The first object prior is that humans perceive the world in terms of objects, or groups of percepts that behave similarly across time and tend to maintain their shape and size Spelke [1990]. We incorporate this prior by developing an object-based probabilistic model of environments and tasks. We provide an algorithm for MLE inference on the parameters of this environment. If two low-level objects are part of the same high level object and therefore have the same behavior, then their dynamics and reward behavior can be modelled by a single model just as well as by individual models for each object. Our inference algorithm formalizes this observation by attempting to combine similar objects together and evaluating the likelihood of a combination via the likelihood of reward and dynamics models trained on the resulting object representation.

Learning causality in sparse reward settings is a fundamental challenge in reinforcement learning. The second human object prior we use is that objects interact only when contacting (Spelke [1990]). We implement this prior by defining an object-contact state representation, reinforcement learning algorithm, and approximation architecture. We represent the state of each object by the object's position, velocity, acceleration, and relative positions, velocities, and accelerations of contacting objects. This representation is both compact and sparse. Our reinforcement learning algorithm calculates discounted returns using a discount factor that is a function of the object state representation, specifically using a lower γ when objects contact, giving these states more credit for future rewards than states where no objects are

¹Paul G. Allen School of Computer Science and Engineering, University of Washington, Seattle, Washington, USA. Correspondence to: William Agnew <wagnew3@cs.washington.edu>, Pedro Domingos <pedrod@cs.washington.edu>.

contacting. Our approximation architecture, which learns to generalize the decisions of the reinforcement learning architecture, consists of simple, sample-efficient models which learn value and reward as a function of which objects are contacting, and richer models that learn value and reward as a function of both which objects are contacting and how those objects are contacting.

The object-contact focused reinforcement learning we propose enables rapid learning of which objects should contact and how, but offers no advantages in states where no objects are contacting. We solve this by using the learned object dynamics models to plan towards states in which contacts occur. However, this planning can be computationally expensive. Our final object prior is that the distance between two objects must decrease for those objects to contact. While simple, this prior allows us to develop planning heuristics which greatly improve the computational efficiency of existing planning algorithms.

We combine these priors into a new reinforcement learning algorithm to create an Object-Level Reinforcement Learner (OLRL). We compare OLRL with humans, deep reinforcement learners, and an object feature set, Blob-PROST (Liang et al. [2016]) on Atari environments, and show that it yields large improvements in sample and computational efficiency. Currently deep reinforcement learning research is often resource and time intensive due to the huge number of experiences needed. Our object detection and tracking module can be used as a general preprocessor for reinforcement learning, greatly increasing the pace and sample efficiency of experiments in this area.

Our contributions are using the following human object priors to create a novel OORL algorithm:

1. Prior of common destiny: percepts that behave the same—same dynamics, value, and reward behavior—are the same and may be treated as one object. We use this prior to build an algorithm that quickly learns a succinct object representation of the environment with no supervision.
2. Object contact prior: objects interact primarily when in contact. Therefore the value and reward functions may be modelled well using object contacts as features. This feature set is small and often has little variance; that is, object contact states change infrequently, enabling sample-efficient learning.
3. Object dynamics prior: the world can be modelled well using classical object dynamics—objects and their positions, velocities, accelerations, and contacts. Using this prior we rapidly learn a forward dynamics model accurate enough to enable effective planning.
4. Implementing these priors into an agent that is more sample efficient than humans on a subset of Atari environments.

2. Related Work

There has been much work on model-based deep reinforcement learning and predicting future states or values with deep networks. Oh et al. [2015] and Chiappa et al. [2017] use deep neural networks to accurately predict Atari frames hundreds of steps into the future. However, these works rely on hundreds of thousands of training frames and computationally intensive deep architectures, do not consider environment stochasticity, and predict at the pixel level rather than the more efficient object level. Kaiser et al. [2019] integrate similar pixel-level frame prediction for Atari into a deep RL agent. Garnelo et al. [2016] use reinforcement learning on a high-level symbolic world representation learned with no supervision, but must still learn what good world representations are and are only successful on very simple environments. Xue et al. [2016], Ebert et al. [2017], Oh et al. [2017], Higuera et al. [2018] all learn to predict future state, but still predict either very low-level features that are difficult to learn on or high-level features that require many samples to effectively model.

Object state representations for reinforcement learning were proposed by Diuk et al. [2008] with a formal framework for describing and reasoning about object interactions. Scholz et al. [2014] extended this framework with physics models of object dynamics. Li et al. [2017] investigate integrating object information into modern deep learning approaches. Kansky et al. [2017] learn more general probabilistic object models and demonstrate how to plan on such models using inference. By learning the parameters of physics-based environments models, Woof and Chen [2018] develop an object embedding network to achieve great performance in complex environments. In contrast to our object recognition algorithm, all of these techniques require environment-specific object labels.

Liang et al. [2016], Machado et al. [2018], Naddaf [2010] begin to tackle the problem of recognizing objects without extensive supervision or hand crafted, object specific recognition algorithms by introducing Blob-PROST, BASS, and DISCO, two large feature sets built by dividing the environment into grids and looking at monocolored blobs. Several recent works, MOREL Goel et al. [2018], OODP Zhu et al. [2018], IODINE Greff et al. [2019], OP3 Veerapaneni et al. [2019], ST-DIM Anand et al. [2019], Transporter Kulkarni et al. [2019], SPACE Lin et al. [2020] present unsupervised techniques for segmenting and modeling objects using deep neural networks. These works use the prior that the observed changes between successive frames can be explained by translations of groups of pixels. Our object segmentation, tracking, and modelling incorporates more knowledge about objects, including object permanence and notions that the pixels composing each object are connected and visually similar. Another key contribution of our work is using not

only object dynamics but also rewards to learn our object representation. For these reasons, our object representations are both more compact and are learned after hundreds, as opposed to tens or hundreds of thousands, of observations. Most critically, we develop an explicit object representation in terms of object positions, velocities, accelerations, and contacts and use this representation for our reinforcement learning. Finally, we also use our object models to plan and incorporate object priors into our value and reward estimators.

Reward shaping is another way to incorporate human priors into reinforcement learning Ng et al. [1999]. Hybrid Reward Architectures Van Seijen et al. [2017] show the potential of object-level reinforcement learning by using per-object reward functions to achieve up to 400x the score of Rainbow Hessel et al. [2018], a state-of-the-art model-free agent, but rely on humans to label objects in its domain, Ms. Pacman.

3. Background

Reinforcement learning solves the problem of taking actions in some environment to maximize some reward. Formally, let $a \in A$ be actions, $s \in S$ be environment states, $t \in 0, 1, \dots, \infty$ be time steps, $G(s', s, a) = P(s'|s, a)$ be a stochastic transition function, $R(s, a)$ be a stochastic reward function, and $\gamma \in [0, 1]$ be a discount factor. These define a Markov decision process where the goal at each time t is to take the action a_t that maximizes the expected discounted reward, $\sum_{t=0}^{\infty} \gamma^k R(s_{t+k}, a_{t+k})$. Each observed (s, a, r, s') tuple is called an experience. Reinforcement learning solves this problem by learning a policy π which specifies the probability of the agent choosing each action given the current state. Define the state value function to be $V_{\pi}(s) = E_{\pi}[\sum_{k=0}^{\infty} \gamma^k R(s_{t+k}, a_{t+k}) | s_t = s]$ and the state-action value function to be $Q_{\pi}(s, a) = E_{\pi}[\sum_{k=0}^{\infty} \gamma^k R(s_{t+k}, a_{t+k}) | s_t = s, a_t = a]$, where $E_{\pi}[\cdot]$ denotes the expected value of the random variable given that the agent follows π . Then the optimal state value and state-action value functions are $V_{*}(s) = \max_{\pi} V_{\pi}(s)$ and $Q_{*}(s, a) = \max_{\pi} Q_{\pi}(s, a)$ for all $s \in S$ and $a \in A$, and an optimal policy π is one that is greedy with respect to the optimal state value or state-action value function.

In model-based reinforcement learning the agent learns a model of the world, and uses this model to plan actions to take or to simulate an environment to learn in. Specifically, the agent learns an approximation of $G(s', s, a)$, the transition function, and $R(s, a)$, the reward function. Intuitively, the better these models are, the better the resulting policy will be. One approach to improving these models is creating a better state representation. That is, rather than learn to predict the state and reward in terms of $s \in S$, learn a map into a smaller state space $h : S \rightarrow S'$, and learn models in this smaller state space. Intuitively, if $|S'|$ is much less

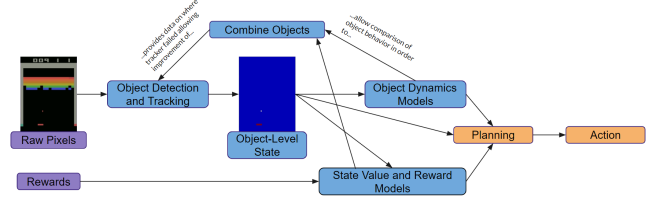


Figure 1: Diagram of OORL framework

than $|S|$ while preserving important features, better models can be learned with the same amount of experience. One general approach to this work is state aggregation Bertsekas [2018], which examines when two states $s_1, s_2 \in S$ may be combined into a single state s_3 , creating a smaller state representation. For tasks where the observations are images or video, h is often thought of as a perception algorithm, processing images into meaningful visual features. Work in this area includes encoder-decoders Oh et al. [2015], Xue et al. [2016], Ebert et al. [2017], Chiappa et al. [2017], Kaiser et al. [2019], object-like feature sets Liang et al. [2016], Machado et al. [2018], Naddaf [2010], object keypoints Kulkarni et al. [2019], and pixel masks of objects Goel et al. [2018], Zhu et al. [2018], Veerapaneni et al. [2019], Greff et al. [2019], Anand et al. [2019], Lin et al. [2020].

4. Model

We extend this work by using object priors to build a powerful object state representation that enables sample efficient and accurate dynamics and reward modelling. We learn our object state representation by jointly maximizing the likelihood of both the world model and the reward model, closing the loop and allowing reinforcement learning to guide perception. Guiding perception to optimize both reward and dynamics modelling has several intuitive advantages. Reward signal is typically very sparse, while predicting dynamics provides a rich signal sufficient for supervised learning. However, learning perception based on purely visual loss can result in distractors in the representation or ignoring objects that differ little from the background visually but provide reward. Considering the value and rewards of objects solves these problems.

We do this by proposing a probabilistic object based model of environments in Table 1 Equation 1, describing how both observations and rewards are generated by a set of objects. Let I^t be an $X \times Y$ image observation of an environment at time t . Our agent divides images into objects, each object o is a set of pixels. $o^t = \{p_0^t, p_1^t, \dots\}$ is the object o at time t , where p are pixels. The existence of o at time t is given by the boolean $e_{o,t}$. The set of all objects the agent can perceive is O . The set of all objects the agent can perceive, as they have been most recently perceived is O_c , and o_l

is o at the most recent time it was present. $F(O)$ are the features an agent observes about each object in the set O , specifically position, velocity, acceleration, and contacts. $F(O)^T$ is the sequence of features observed about O during the set of times T . D is a learned environment model. Let $D_{o,v}$, $D_{o,e}$, $D_{o,c}$, $D_{o,p}$ be the models for the velocity of o , when o exists, where o appears when it starts existing, and the pixels composing o , respectively. $D_{o,v}$ and $D_{o,p}$ take a^{t-1} and $F(o^{t-1})$ as inputs, and $D_{o,e}$ and $D_{o,c}$ take a^{t-1} and $F(O^{t-1})$ as inputs. Let $D_{o,\cdot}(o^t)$ be the prediction of $D_{o,\cdot}$ on $F(o^t)$ and a^t . r^t is the reward the agent receives at time step t . R_O and V_O are a reinforcement learning algorithm which is trained on $F(O)^{T_{\text{train}}}$ and $r^{T_{\text{train}}}$ to predict the rewards and value, respectively, of a state at time t given $F(O^t)$ and a^t .

We model the observations of the environment as being generated by an MDP over objects, their dynamics, and rendering objects into pixels. Given a set of observations $I = \{I^0, I^1, \dots, I^T\}$ containing n objects $\{o_0, o_1, \dots, o_n\} = O$ properties (shape, color, mass, etc) $\{p_0, p_1, \dots, p_n\} = P$ and associated dynamics d . Each object o at each time t has a state $F(o^t) = s_{o,t}$ comprising its properties and position, velocity, acceleration, contact status, and whether it currently exists. Let $S_t = \{s_{o,t} \mid \forall o \in O\}$. In Table 1 we give $P(I)$, the distribution of environment observations. Rendering is assumed to choose uniformly at random one of the pixels among those with the same coordinates to render, and object properties are domain specific.

We use the prior that objects provide a succinct and powerful model of the world and the prior that objects only interact when in contact to develop the object contact state representation s which we parameterize our dynamics and rewards models (Equations 3-7) with. Given an object o , the corresponding object contact feature set s_o is the position, velocity, and acceleration of o , and the relative position, velocity, and accelerations of any objects o' that o is in contact with. Using these two priors, we develop a small, sparse, but powerful feature set to model reward and dynamics with. We use prior that simpler environments with fewer objects are more likely to derive Equation 2, modelling the number of objects with a geometric distribution. Finally, we use the prior that objects behave consistently across time by having our dynamics and reward models characterizations be only a function of the current state and action in Equations 3-7. While simple, this prior forms the core of our inference algorithm, where we search for objects with very similar dynamics and reward behavior and combine them together to create a more likely (and succinct) object representation.

5. Inference

In this section we describe how we compute the MLE set of parameters for this model. Our model is parameterized

by O , the set of objects our agent divides the world into, with O^t being the objects and associated properties (pixels, position, velocity, acceleration, contact status) at time t , D , the learned dynamics model of the objects and R_O , the learned value and reward model over object features. The likelihood of these parameters is:

$$L(O, D, R_O) = b(1-b)^{|O|-1} \prod_{t \in T_t} P(R_O(s^t, a^t) = r_t) \\ \times \prod_{c \in X, Y} \frac{\sum_{o \in O^{t-1}} \sum_{c' \in X, Y} P(D_{o,v}(o) + c' = c) P(D_{o,p}(o) = I^t(c))}{\sum_{o \in O^{t-1}} \sum_{c' \in X, Y} P(D_{o,v}(o) + \langle c' \rangle = \langle x, y \rangle)}$$

Rather than compute likelihood based on the pixel observations, we may initialize with a segmentation algorithm S , tuned to always oversegment, so no two true objects are segmented together, and tracking algorithm T , tuned to always undertrack, so T never produces false positive trackings. We use S to segment each image and T to greedily assign trackings to create an initial set of objects, or percepts, P . Doing so allows incorporation of prior knowledge and algorithms and further improves sample efficiency of our algorithm. In this case, the likelihood is in terms of reconstructing the positions of the initial objects:

$$L_S(O, D, R_O) = b(1-b)^{|O|-1} \prod_{t \in T_t} P(R_O(s_t, a^t) = r_t) \\ \times \prod_{p \in P^t} P(D_{o_p,e}(o_p^{t-1}) = 1) P(D_{o_p,v}(o_p^{t-1}) = v(p^t)) P(D_{o_p,c}(o_p^{t-1})(p) = p^t)$$

Where o_p is the object p was previously mapped to, and $v(p^t)$ is the velocity of p from time $t-1$ to t . We approximate MLE object segmentation as follows. Given two objects, $o_1, o_2 \in O$, we combine them together to form a new object $o_3 = \{o_1, o_2\}$ and object map $O' = (O \setminus \{o_1, o_2\}) \cup o_3$. If o_1 and o_2 appear disjoint times, then when our segmentation transitions between the two objects is an instance where our tracking algorithm failed. Using this observation, we obtain supervised data for when T fails, and we use this data to learn a better tracking algorithm. We compare the likelihoods of O and O' and accept O' as the new object representation if it is more likely. We may also attempt to split an object, $o_3 = \{o_1, o_2\}$, into two separate objects, o_1 and o_2 , by similarly compare the likelihoods of the corresponding object representations. We detail this procedure in Algorithm 1. Our agent processes each frame into an object representation by using S to oversegment the image, then T_L , a learned tracking algorithm, to track segments into past objects, and finally O to combine these object primitives into high level objects. We detail this in Algorithm 2 in the appendix.

6. Learning

In this section we describe our model based reinforcement learning algorithm. Our agent learns a dynamics model

```

1  Choose  $o_1, o_2 \in O \cup S$ , or  $o_1 \in O$  and  $o_2 \in S$  s.t.  $o_2 \in o_1$ 
2  if  $o_2 \in o_1$  then
3       $o_3 = o_1 \setminus o_2$  ▷ Make split object
4       $O' = O \setminus o_1$  ▷ Make new object set
5       $O' = O' \cup o_3$ 
6      Train  $D_{O'}$  ▷ Train dynamics models for new objects
7      Train  $R_{O'}$  ▷ Train value model for new object set
8      if  $\log L(O', D_{O'}, R_{O'}) \geq \log L(O, D_O, R_O)$  then
9          Train  $T_L$  ▷ Train new tracker
10          $O = O'$  ▷ Split object
11     end
12 end
13 else
14      $o_3 = o_1 \cup o_2$  ▷ Make combined object
15      $O' = O \setminus \{o_1, o_2\}$  ▷ Make new object set
16      $O' = O' \cup o_3$ 
17     Train  $D_{O'}$ 
18     Train  $R_{O'}$  ▷ Train value model for new object set
19     if  $\log L(O', D_{O'}, R_{O'}) \geq \log L(O, D_O, R_O)$  then
20         if  $\{t|o_1 \in O^t\} \cap \{t|o_2 \in O^t\} = \emptyset$  then
21             foreach  $(o_1^t, o_2^t) | t' > t, o_1, o_2 \notin$   

22                  $O^{t+1:t'-1}, (o_1^t, o_2^t) \in H$  do  

23                 |  $M((o_1^t, o_2^t)) = 1$  ▷ Correct tracker  

24             end
25             foreach  $(o_2^t, o_1^t) | t' < t, o_1, o_2 \notin$   

26                  $O^{t'+1:t-1}, (o_2^t, o_1^t) \in H$  do  

27                 |  $M((o_2^t, o_1^t)) = 1$  ▷ Correct tracker  

28             end
29             Train  $T_L$  ▷ Train new tracker
30         end
31          $O = O'$  ▷ Combine objects
32     end
33 end

```

dimension $d \in D$, an *appearance model*, $D_{o,a,d}$ is trained to output a probability vector over the possible locations of o in dimension d when $D_{o,e}$ predicts o will appear given the current positions, velocities, accelerations, and contacts of all objects. A *velocity model*, $D_{o,v,d}$ is trained to output a probability vector over the possible future velocities of o in dimension d in the next time step given the absolute and relative positions, velocities, and accelerations and contacts of o . We split timesteps into two sets, T_{train} and T_{infer} , for training dynamics and reward models and inferring the MLE object representation, respectively.

Value and Reward Estimation—We use on-policy Monte Carlo control (Sutton [1988]) to estimate Q values. We then train models V_O to predict Q value and R_O to predict reward given the current state, $F(O^t)$ and next action, a^t . We use the prior that objects interact when they contact into reinforcement learning to derive contact discounted return. The contact discounted return is calculated using two decay rates: γ_{nc} for states where no objects are contacting, and γ_c for states where objects are contacting, with $\gamma_{nc} > \gamma_c$. Since $\gamma_{nc} > \gamma_c$, from the backward view the agent assigns more credit for reward to recent object contacts, and in the forward view only considers the next few object contacts when deciding how to act.

We also use a contact-focused model architecture and feature set for approximating values and rewards. R and V are learned as an ensemble of models, one for each pair of objects $o_1, o_2 \in O$.

$$R_{O,o_1,o_2}(F(O^t)) = \bar{r}_{c,o_1,o_2} + R_{M,o_1,o_2}(F(o_1), F(o_2), F(o_1, o_2))$$

$$V_{O,o_1,o_2}(F(O^t)) = \bar{v}_{c,o_1,o_2} + R_{V,o_1,o_2}(F(o_1), F(o_2), F(o_1, o_2))$$

where \bar{r}_{c,o_1,o_2} and \bar{v}_{c,o_1,o_2} are the average reward and value, respectively, when o_1 and o_2 are contacting, $F(o_1, o_2)$ are the relative position, velocity, and acceleration between o_1 and o_2 , and R_M and V_M are learned models trained to minimize the error of R_{O,o_1,o_2} and V_{O,o_1,o_2} on states where o_1 and o_2 are in contact. By estimating value and reward by ensembling mean estimation with more complex models, R_M and V_M , these R_O and V_O quickly learn which objects are good and bad to contact, which is often sufficient to create a reasonably good policy. More complex interactions are learned by the richer models R_M and V_M .

Planning and Action Selection—Our estimators assume reward and value are zero unless objects are contacting. One difficulty this poses is determining which action to take when no objects are contacting. This may be solved by planning into the future until object contacts are encountered, but planning is often computationally expensive given that the number of possible action sequences grows exponentially. Closely following Ng’s work on reward shaping (Ng et al. [1999]), we shape our reward and value functions by transforming them into potentials with respect to the distances

between object pairs and adding these potentials to the original reward and value functions. This can be interpreted intuitively as incorporating the prior that to make two objects contact the distance between those two objects should be decreased, and vice versa. Using this shaped reward, we plan using UCT tree search. (Browne et al. [2012]).

7. Implementation

We use XGBoost trees to learn our dynamics and value models, D and V_M , and a neural network to learn our reward model, R_M . We do not learn a model of object properties; instead we assume that object properties do not change, an approximation that we found does not impact performance. We provide more implementation details and hyperparameters in the appendices.

8. Experiments and Results

In this section we demonstrate that our object-level framework is capable of creating succinct and accurate object-level models on a variety of Atari games with very few sample. We then compare our OLRL agent against DQN, Blob-PROST, and humans. Our method of combining low-level percepts by searching for smaller yet still accurate models reduces the number of objects from dozens to a core few, as shown in Figure 3.

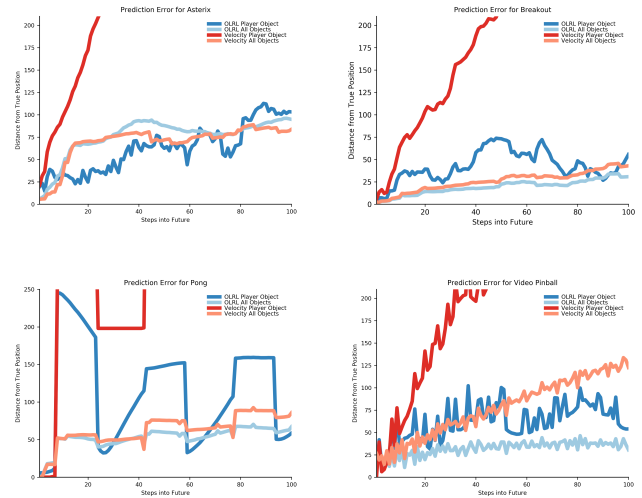


Figure 2: Model Error on Atari Environments. Distances are in pixels; for comparison, the Atari observation is 210x160 pixels.

World Model Analysis—We demonstrate the speed and accuracy of our object-level perception and modeling on a variety of Atari 2600 games. For each Atari game, we trained our model for only 2000 steps, where each step is 4

game frames, collected while playing random actions. We then evaluated our models by first playing n random actions, where n was sampled uniformly from $[50, 150]$, and then predicting the positions of objects for the next 100 steps. Figure 2 shows prediction error as the average Euclidean distance between the predicted and actual object positions. Since many Atari objects do not move, we also show prediction error for the player-controlled object, which has complex dynamics. For the same reason, we use predicting that object velocity will remain constant as a natural baseline. Even with very little training data, our models have learned object dynamics with high accuracy tens of frames into the future, effective for short-term planning. In addition, model prediction error generally does not explode for longer prediction horizons, allowing the agent to consider the approximate positions over objects even 100 steps into the future.

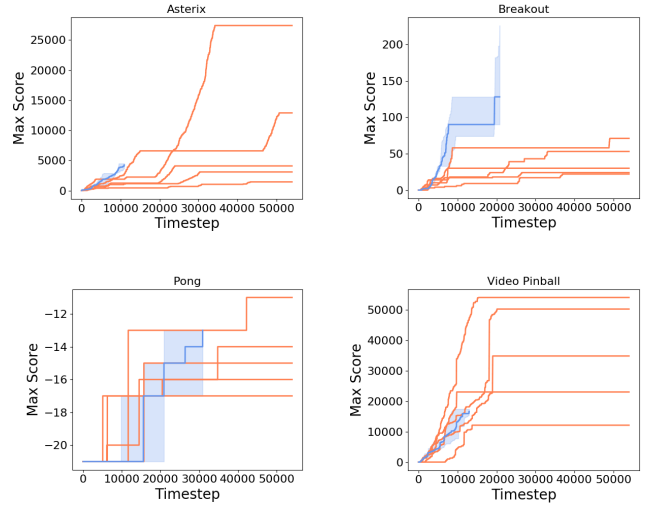


Figure 4: Comparison of OLRL and human learning curves on Atari games. Each human learning curve shown in red. Median OLRL score and error bars shown in blue.

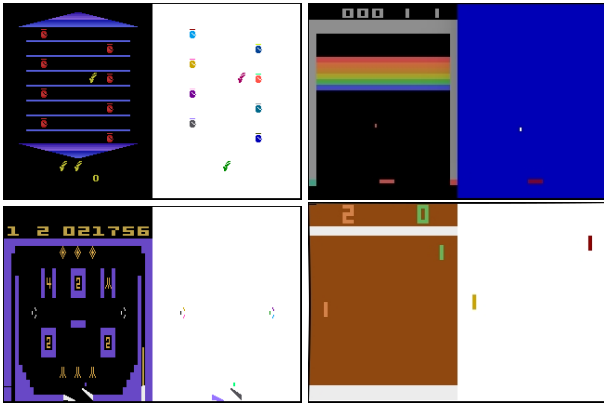


Figure 3: Object-level representations of Atari games. Left: normal Atari game frames. Right: same frame with each high-level object our agent perceives colored differently.

Comparison to Humans—We compare the maximum scores achieved by each time step for humans and OLRL in Figure 4. For all games tested, this value plateaus for humans, indicating they are not increasing their highest score and have saturated learning. Given just minutes of training data, OLRL is able to outperform humans learning for 15 minutes 65% of the time. We say that OLRL learns faster than a human if OLRL reaches this maximum score in fewer time steps than the human. OLRL is able to learn faster than humans 55% of the time, demonstrating the power of the object heuristics we have incorporated. This is despite humans having extensive prior knowledge, particularly for environments like Video Pinball.

Comparison to Deep RL—We compare OLRL to DQN and Blob-PROST in Figure 5. DQN and Blob-PROST data was drawn from Machado et al. [2018]. Using our object-level features, our agent reaches equivalent or greater performance than DQN and Blob-PROST with approximately 10,000x fewer experiences in three of the four games. Although DQN and Blob-PROST outperform OLRL in Pong, they require over 100x more experiences to reach the performance of OLRL. Furthermore, SimPLe Kaiser et al. [2019], the current state of the art for Atari in sample-limited regimes, achieves a mean of 54% the human-normalized score across Pong, Asterix, and Breakout after 100,000 steps; our agent achieves a mean of 176% human normalized score with fewer than 10,000 steps.

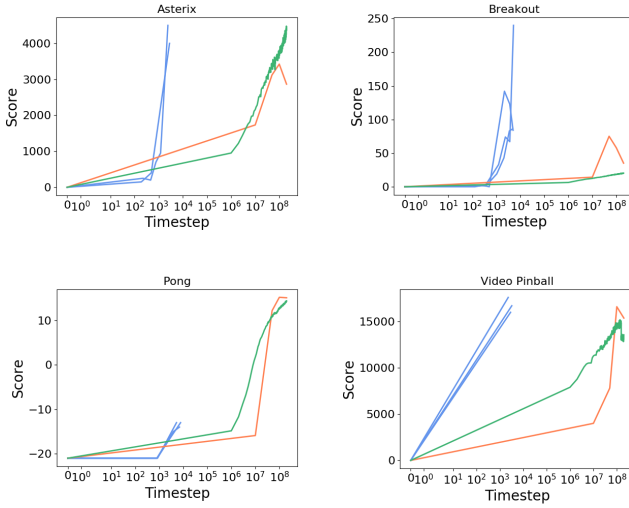


Figure 5: Comparison of OLRL, DQN, and Blob-PROST. Blue: OLRL, green: Blob-PROST, red: DQN. Note time steps are in log-scale.

Robustness—Object-level representations are inherently robust to changes in object appearance within the limits of the object tracking algorithm used. Our OLRL framework further improves robustness in an additional way. Aggregating objects with similar appearances is often a good heuristic, but, as stated in Oh et al. [2015], preservation of dynamics and reward are sufficient conditions for aggregation. OLRL uses object appearance to help select candidate objects for aggregation, but chooses to aggregate solely based on preservation of dynamics and reward. Explicitly excluding object appearance from aggregation decisions makes OLRL highly robust to even dramatic changes in object appearance. In Figure 6, we train OLRL for 10,000 time steps and DQN for 50 million time steps on Breakout. Then we test robustness by changing the background color from black to white. Even though OLRL’s tracking model fails to track the background after its color is changed and perceives the background as a new object, OLRL is able to quickly recover to previous performance levels by modelling the behavior of the new object and quickly combining it with the original background object.

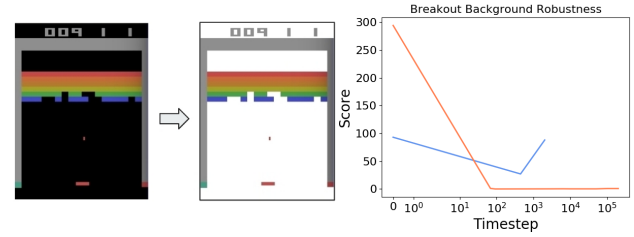


Figure 6: Robustness analysis. Left: change in Breakout environment. Right: learning curve for OLRL (blue) and DQN (red) after change in environment.

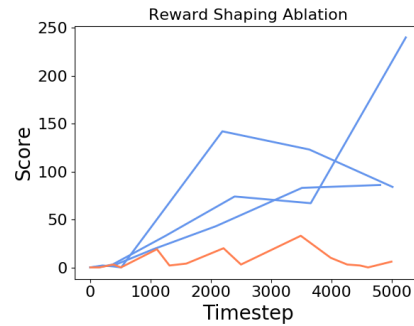


Figure 7: Ablation for our contact discounted return on Breakout. OLRL with reward shaping in blue, OLRL without reward shaping in red.

Ablations—In Figure 7 we provide an ablation for our reward shaping for planning. Achieving a high score in Breakout requires planning many steps ahead to contact a ball. Without using reward shaping to extend the learned contact reward and value to adjacent states, the agent is unable to effectively plan action sequences to reach the ball.

Interpretability—Our learned policy is easily interpretable: the agent will try to contact objects with value and reward higher than the background, and avoid those objects with value and reward lower than the background. For example, in the game Breakout, the goal is to hit a ball with a paddle. After training an OLRL agent on Breakout, we find that contacts between the ball and paddle have an average value of 0.147 and average reward of 0 and contacts between the paddle and background have an average value of 0.139 and average reward of 0.007, providing a clear explanation for why the OLRL agent correctly favors contacting the ball with the paddle over the background.

9. Conclusion

This work provides an exciting demonstration of the potential of human object priors for reinforcement learning.

Using these priors, we develop an object inference algorithm that closes the loop on perception and reinforcement learning by finding the set of objects that jointly maximizes the likelihood of the dynamics and the reward models. We also use object-contact priors to develop a novel discounting scheme that better captures causality, and motivate reward shaping to make planning more efficient. On the subset of Atari environments we evaluate on, our agent learns 10,000x faster than classical deep RL algorithms and better than state of the art deep RL algorithms for sample-limited regimes. Our agent is even able to learn in fewer environment interactions than humans. Finally, our object representation gives promising robustness and interpretability results, two problems of growing interest for the community.

In this work we initialized our object distribution with simple classical tracking and segmentation algorithms. In future work we would like to use powerful deep segmentation and tracking algorithms to extend our results to realistic 3D environments. We believe a compact and explicit object representation paves the way for new results in robustness and new ideas in exploration, transfer learning, specifically learning relations between objects, and interpretability.

10. Acknowledgements

This work was supported by an NDSEG Fellowship and ONR grant N00014-18-1-2826. The GPU machine used for this research was donated by Nvidia.

References

- Elizabeth S Spelke. Principles of object perception. *Cognitive Science*, 14(1):29–56, 1990.
- Volodymyr Mnih, Koray Kavukcuoglu, David Silver, Andrei A Rusu, Joel Veness, Marc G Bellemare, Alex Graves, Martin Riedmiller, Andreas K Fidjeland, Georg Ostrovski, et al. Human-level control through deep reinforcement learning. *Nature*, 518(7540):529, 2015.
- Volodymyr Mnih, Adria Puigdomenech Badia, Mehdi Mirza, Alex Graves, Timothy Lillicrap, Tim Harley, David Silver, and Koray Kavukcuoglu. Asynchronous methods for deep reinforcement learning. In *International Conference on Machine Learning*, pages 1928–1937, 2016.
- David Silver, Julian Schrittwieser, Karen Simonyan, Ioannis Antonoglou, Aja Huang, Arthur Guez, Thomas Hubert, Lucas Baker, Matthew Lai, Adrian Bolton, et al. Mastering the game of go without human knowledge. *Nature*, 550(7676):354, 2017.
- Carlos Diuk, Andre Cohen, and Michael L Littman. An object-oriented representation for efficient reinforcement learning. In *International Conference on Machine Learning*, pages 240–247. ACM, 2008.
- Jonathan Scholz, Martin Levihn, Charles Isbell, and David Wingate. A physics-based model prior for object-oriented mdps. In *International Conference on Machine Learning*, pages 1089–1097, 2014.
- Vikash Goel, Jameson Weng, and Pascal Poupart. Unsupervised video object segmentation for deep reinforcement learning. In *Advances in Neural Information Processing Systems*, pages 5688–5699, 2018.
- Guangxiang Zhu, Zhiao Huang, and Chongjie Zhang. Object-oriented dynamics predictor. In S. Bengio, H. Wallach, H. Larochelle, K. Grauman, N. Cesa-Bianchi, and R. Garnett, editors, *Advances in Neural Information Processing Systems 31*, pages 9804–9815. Curran Associates, Inc., 2018.
- Klaus Greff, Raphaël Lopez Kaufmann, Rishab Kabra, Nick Watters, Chris Burgess, Daniel Zoran, Loic Matthey, Matthew Botvinick, and Alexander Lerchner. Multi-object representation learning with iterative variational inference. *arXiv preprint arXiv:1903.00450*, 2019.
- Zhixuan Lin, Yi-Fu Wu, Skand Vishwanath Peri, Weihao Sun, Gautam Singh, Fei Deng, Jindong Jiang, and Sungjin Ahn. Space: Unsupervised object-oriented scene representation via spatial attention and decomposition. *arXiv preprint arXiv:2001.02407*, 2020.
- Yitao Liang, Marlos C Machado, Erik Talvitie, and Michael Bowling. State of the art control of atari games using shallow reinforcement learning. In *Proceedings of the 2016 International Conference on Autonomous Agents & Multiagent Systems*, pages 485–493. International Foundation for Autonomous Agents and Multiagent Systems, 2016.
- Junhyuk Oh, Xiaoxiao Guo, Honglak Lee, Richard L Lewis, and Satinder Singh. Action-conditional video prediction using deep networks in atari games. In *Advances in Neural Information Processing Systems*, pages 2863–2871, 2015.
- Silvia Chiappa, Sébastien Racaniere, Daan Wierstra, and Shakir Mohamed. Recurrent environment simulators. *arXiv:1704.02254*, 2017.
- Lukasz Kaiser, Mohammad Babaeizadeh, Piotr Milos, Blazej Osinski, Roy H Campbell, Konrad Czechowski, Dumitru Erhan, Chelsea Finn, Piotr Kozakowski, Sergey Levine, et al. Model-based reinforcement learning for atari. *arXiv preprint arXiv:1903.00374*, 2019.
- Marta Garnelo, Kai Arulkumaran, and Murray Shanahan. Towards deep symbolic reinforcement learning. *arXiv:1609.05518*, 2016.
- Tianfan Xue, Jiajun Wu, Katherine Bouman, and Bill Freeman. Visual dynamics: Probabilistic future frame syn-

- thesis via cross convolutional networks. In *Advances in Neural Information Processing Systems*, pages 91–99, 2016.
- Frederik Ebert, Chelsea Finn, Alex X Lee, and Sergey Levine. Self-supervised visual planning with temporal skip connections. In *Conference on Robot Learning*, pages 344–356, 2017.
- Junhyuk Oh, Satinder Singh, and Honglak Lee. Value prediction network. In *Advances in Neural Information Processing Systems*, pages 6120–6130, 2017.
- Juan Camilo Gamboa Higuera, David Meger, and Gregory Dudek. Synthesizing neural network controllers with probabilistic model-based reinforcement learning. In *2018 IEEE/RSJ International Conference on Intelligent Robots and Systems (IROS)*, pages 2538–2544. IEEE, 2018.
- Yuezhang Li, Katia Sycara, and Rahul Iyer. Object-sensitive deep reinforcement learning. *EPiC Series in Computing*, 50:20–35, 2017.
- Ken Kanksy, Tom Silver, David A Mely, Mohamed Eldawy, Miguel Lázaro-Gredilla, Xinghua Lou, Nimrod Dorfman, Szymon Sidor, Scott Phoenix, and Dileep George. Schema networks: Zero-shot transfer with a generative causal model of intuitive physics. In *International Conference on Machine Learning*, pages 1809–1818, 2017.
- William Woof and Ke Chen. Learning to play general video-games via an object embedding network. In *2018 IEEE Conference on Computational Intelligence and Games (CIG)*, pages 1–8. IEEE, 2018.
- Marlos C Machado, Marc G Bellemare, Erik Talvitie, Joel Veness, Matthew Hausknecht, and Michael Bowling. Revisiting the arcade learning environment: Evaluation protocols and open problems for general agents. *Journal of Artificial Intelligence Research*, 61:523–562, 2018.
- Yavar Naddaf. Game-independent ai agents for playing atari 2600 console games. Master’s thesis, University of Alberta, 2010.
- Rishi Veerapaneni, John D Co-Reyes, Michael Chang, Michael Janner, Chelsea Finn, Jiajun Wu, Joshua B Tenenbaum, and Sergey Levine. Entity abstraction in visual model-based reinforcement learning. *arXiv preprint arXiv:1910.12827*, 2019.
- Ankesh Anand, Evan Racah, Sherjil Ozair, Yoshua Bengio, Marc-Alexandre Côté, and R Devon Hjelm. Unsupervised state representation learning in atari. In *Advances in Neural Information Processing Systems*, pages 8766–8779, 2019.
- Tejas D Kulkarni, Ankush Gupta, Catalin Ionescu, Sebastian Borgeaud, Malcolm Reynolds, Andrew Zisserman, and Volodymyr Mnih. Unsupervised learning of object keypoints for perception and control. In *Advances in Neural Information Processing Systems*, pages 10723–10733, 2019.
- Andrew Y Ng, Daishi Harada, and Stuart Russell. Policy invariance under reward transformations: Theory and application to reward shaping. In *International Conference on Machine Learning*, 1999.
- Harm Van Seijen, Mehdi Fatemi, Joshua Romoff, Romain Laroche, Tavian Barnes, and Jeffrey Tsang. Hybrid reward architecture for reinforcement learning. In *Advances in Neural Information Processing Systems*, pages 5392–5402, 2017.
- Matteo Hessel, Joseph Modayil, Hado Van Hasselt, Tom Schaul, Georg Ostrovski, Will Dabney, Dan Horgan, Bilal Piot, Mohammad Azar, and David Silver. Rainbow: Combining improvements in deep reinforcement learning. In *Thirty-Second AAAI Conference on Artificial Intelligence*, 2018.
- Dimitri P Bertsekas. Feature-based aggregation and deep reinforcement learning: A survey and some new implementations. *IEEE/CAA Journal of Automatica Sinica*, 6(1):1–31, 2018.
- Richard S Sutton. Learning to predict by the methods of temporal differences. *Machine Learning*, 3(1):9–44, 1988.
- Cameron B Browne, Edward Powley, Daniel Whitehouse, Simon M Lucas, Peter I. Cowling, Philipp Bohnlshagen, Stephen Tavener, Diego Perez, Spyridon Samothrakis, and Simon Colton. A survey of monte carlo tree search methods. *IEEE Transactions on Computational Intelligence and AI in Games*, 4(1):1–43, 2012.
- Pedro F Felzenszwalb and Daniel P Huttenlocher. Efficient graph-based image segmentation. *International journal of computer vision*, 59(2):167–181, 2004.
- Alireza Khotanzad and Yaw Hua Hong. Invariant image recognition by zernike moments. *IEEE Transactions on Pattern Analysis and Machine Intelligence*, 12(5):489–497, 1990.
- Tianqi Chen and Carlos Guestrin. Xgboost: A scalable tree boosting system. In *Proceedings of the 22nd ACM SIGKDD International Conference on Knowledge Discovery and Data Mining*, pages 785–794. ACM, 2016.
- Guolin Ke, Qi Meng, Thomas Finley, Taifeng Wang, Wei Chen, Weidong Ma, Qiwei Ye, and Tie-Yan Liu. Lightgbm: A highly efficient gradient boosting decision tree. In *Advances in Neural Information Processing Systems*, pages 3146–3154, 2017.
- Pedro A Tsividis, Thomas Pouncy, Jacqueline L Xu, Joshua B Tenenbaum, and Samuel J Gershman. Human learning in atari. *Association for the Advancement of Artificial Intelligence*, 2017.

Greg Brockman, Vicki Cheung, Ludwig Pettersson, Jonas Schneider, John Schulman, Jie Tang, and Wojciech Zaremba. Openai gym, 2016.

A. Implementation Details

At a low level, our system works by, at each timestep, perceiving objects, tracking those objects onto past objects, and using the object dynamics, reward, and value models to plan and execute an action. As the agent gathers more experience, the object dynamics, reward, and value models are periodically retrained, and the inference procedure detailed in the main paper is also rerun to find the MLE set of objects. In the next sections we give the technical implementation details and hyperparameters.

A.1. Object Perception and Tracking

We perceive and track objects using Algorithm 1. For the base segmentation algorithm S , we use Felzenszwalb segmentation Felzenszwalb and Huttenlocher [2004] with a scale of 1000 and sigma of 0. For the base tracking algorithm T , we use an ensemble of human-inspired tracking features detailed in Equation 1.

Let $loc(o)$ for $o \in \mathcal{O}$ be the mean coordinates of the pixels composing object o . Consider two objects, o_p observed in a previous experience, and o_c observed in the current experience. We create a tracking score between the two objects as a linear combination of intuitive features:

$$\begin{aligned} T(o_c, o_p) = & w_0 \mathcal{F}_{disp}(o_c, o_p) + w_1 \mathcal{F}_{shape}(o_c, o_p) \\ & + w_2 \mathcal{F}_{disp}(o_c, o_p) \mathcal{F}_{shape}(o_c, o_p) + w_3 \mathcal{F}_{perm}(o_c, o_p) \quad (1) \\ & + w_4 \mathcal{F}_{size}(o_c, o_p) + w_5 \mathcal{F}_{motion}(o_c, o_p) \end{aligned}$$

$\mathcal{F}_{disp}(o_c, o_p)$ is the total change in relative distance between o_c and o_p and all objects contacting o_p , capturing the notion that over small changes in time the positions of objects generally do not change too much.

$$\mathcal{F}_{shape}(o_c, o_p) = \sum_{i=1}^{25} |\log(Z_i(o_c)) - \log(Z_i(o_p))|$$

where $Z_i(o) = i$ th Zernike moment (Khotanzad and Hong [1990]) of o , encoding object shape consistency.

$\mathcal{F}_{perm}(o_c, o_p)$ captures the intuition that objects generally do not appear or disappear and is the number of experiences since o_p was last seen,

$$\mathcal{F}_{size}(o_c, o_p) = \max\left(\frac{|o_c|}{|o_p|}, \frac{|o_p|}{|o_c|}\right) - 1.$$

$\mathcal{F}_{motion}(o_c, o_p)$ encodes that many objects are background objects and are unlikely-move:

$$\mathcal{F}_{motion}(o_c, o_p) = \log(\max(P_{motion}(o_c, o_p), \epsilon)),$$

where ϵ is some small positive constant.

$$P_{motion}(o_c, o_p) = \begin{cases} P_{dm}(\text{Moves}(o_p)|e_1, \dots, e_i), & \text{if } loc(o_c) \neq loc(o_p) \\ P_{dm}(\text{NotMoves}(o_p)|e_1, \dots, e_i), & \text{if } loc(o_c) = loc(o_p) \end{cases}$$

Algorithm 2: Perceive and Track Objects

```

1 Input :  $I^t$ , observation at current timestep
2  $P^t = \{\}$ 
3  $O^t = \{\}$ 
4  $Q = S(I^t)$  ▷ Segment image
5 foreach  $q \in Q$  do
6   foreach  $p \in P_c$  do
7      $H = H \cup (p, q)$  ▷ Add all possible trackings to
8     history
9      $M((p, q)) = T_L(p, q)$ 
10  end
11 while  $\max_{q \in Q, p \in P_c} T_L(p, q) \geq w_t$  do
12    $q, p = \arg \max_{q \in Q, p \in P_c} T_L(p, q)$  ▷ Greedily assign
13   trackings
14    $p_t = q$ 
15    $P^t = P^t \cup \{p^t\}$ 
16    $Q = Q \setminus \{q\}$ 
17 end
18  $O = O \cup Q$  ▷ Add untracked percepts as new objects
19 foreach  $o \in O_c$  do
20   if  $o \subseteq P^t$  then
21      $o^t = \{p^t \in P^t | p^t \in o\}$  ▷ Map percepts to objects
22      $O^t = O^t \cup \{o^t\}$ 
23      $P^t = P^t \setminus o$ 
24   end
25 return  $O^t$ 

```

A.2. Planning

We plan using UCT tree search. We slightly modify the algorithm to evaluate action paths in batches; while this leads to slight suboptimality in action path selection, it leads to significant gains in evaluation speed. We plan with a batch size of 160 for 10 steps, up to plans of 8 actions in length. We use the standard exploration constant of $\frac{1}{\sqrt{2}}$. We select the action to take by applying a softmax transform to the action values with a scale of 4000 and sampling an action from the resulting distribution.

A.3. Learning Dynamics, Value, and Reward Models

Dynamics Models—We model the velocity of each object in each dimension with a separate XGBoost Chen and Guestrin [2016] tree. Each tree outputs a probability vector over velocities, discretized in steps of 1 between -30 and 30. Each

tree is trained to minimize multiclass logloss, has a maximum depth of $\max(2, \min(6, |D|/50))$, where D is the size of the training data. Experiences are split into a 80:20 train/validation split, which is used for early stopping of training (5 rounds), and for computing the model likelihoods used in the Infer algorithm in the main paper. Where objects appear when they transition from not being present to being present is modelled with an XGBoost tree per object per dimension trained to output a probability vector over positions. Each tree has a maximum depth of 6 and is trained to minimize multiclass logloss, with a similar 80:20 train/validation data split. Object presence is modelled with an XGBoost tree per object, minimizing multiclass logloss on an 80:20 split with a maximum tree depth of 6. For all models, mean prediction was also evaluated, and if mean prediction yields better validation error it was used instead (we did this primarily to prevent objects with very little associated data from causing noisy validation error behavior in the XGBoost trees and interfering with the Infer algorithm).

Reward and Value Models—Our agent uses Monte Carlo Control Sutton [1988] with a discount factor of 0.99 to estimate state-action values. We then learn to predict state-action reward and value with sets of ensemble models for each object pair. Each ensemble model has two parts: the first is simple mean estimation of the reward or value for when the objects are in contact. The second is an XGBoost tree trained to predict value or reward given the absolute and relative positions, velocities, accelerations, and contact states of the object pair. Each tree was trained to predict the mean of a Gaussian distribution with variance 1 describing the reward distribution for each state-action \times object pair and trained to maximize likelihood. Data was split into 75:25 train/validation.

A.4. Tracking Model

We learn a tracking model consisting of two LightGBM Ke et al. [2017] trees. We used LightGBM rather than XGBoost trees because of the large amount of tracking data made the faster training time of LightGBM advantageous. For each object, we trained a lightGBM tree on the negative tracking instances associated with that object and the tracking instance which were once negative but later learned to be positive via the Infer algorithm in the main paper. We used the tracking features described in Appendix A.1 as inputs. The LightGBM tree was trained to output a number between 0 and 1. We form the learned tracking algorithm T_L , by taking the maximum of the base tracking algorithm T , and the learned LightGBM tracking algorithm.

B. Human Atari Learning Data

One of the most exciting achievements of reinforcement learning is outperforming humans Mnih et al. [2015] in

Atari games, and several years later, human normalized score is one of the most important metrics for comparing deep learners Hessel et al. [2018]. Interestingly, this key metric is based off of the performance of one expert human. However, as seen in the data of a recent study on human play in Atari Tsividis et al. [2017], some of these expert scores are beaten after only 15 minutes of play. In addition, the published data do not include learning curves, just the final scores after learning. Motivated by these facts and growing interest in sample efficient reinforcement learning, we conducted our own study of human Atari game play for four games to obtain learning curves. Five participants were tasked with playing Asterix, Breakout, Pong, and Video Pinball for 15 minutes each. To ensure the environment the humans were tested on was identical to the environment we trained our agents on, we used OpenAI Gym Brockman et al. [2016] as the Atari emulator. We found that there is very high variance in score between participants, even on Asterix, which participants were unlikely to have played before. In every game at least one participant was able to beat the expert score in 15 minutes of play, and in all but Pong average maximum participant score exceeded the expert score. We suspect this is because of differences in the Atari emulator used.